


Article

Reactivity of a Sterical Flexible Pentabenzylcyclopentadienyl Samarocene

 Niklas Reinfandt and Peter W. Roesky * 

Institute for Inorganic Chemistry, Karlsruhe Institute of Technology, Engesserstraße 15, 76131 Karlsruhe, Germany; niklas.reinfandt@partner.kit.edu

* Correspondence: roesky@kit.edu

Abstract: Reactivity studies of the classical divalent lanthanide compound $[\text{Cp}^{\text{Bz}5}_2\text{Sm}]$ ($\text{Cp}^{\text{Bz}5}$ = pentabenzylcyclopentadienyl-anion) towards diphenyl dichalcogenides and d-element carbonyl complexes led to remarkable results. In the compounds obtained, a different number of Sm-C(phenyl) interactions and differently oriented benzyl groups were observed, suggesting—despite the preference of these interactions in $[\text{Cp}^{\text{Bz}5}_2\text{Sm}]$ described in previous studies—a flexible orientation of the benzyl groups and thus a variable steric shielding of the metal center by the ligand. The obtained compounds are either present as monometallic complexes (reduction of the dichalcogenides) or tetrametallic bridged compounds in the case of the d/f-element carbonyl complexes.

Keywords: samarium; reduction; pentabenzylcyclopentadienyl; carbonyl complexes; chalcogenides



Citation: Reinfandt, N.; Roesky, P.W. Reactivity of a Sterical Flexible Pentabenzylcyclopentadienyl Samarocene. *Inorganics* **2022**, *10*, 25. <https://doi.org/10.3390/inorganics10020025>

Academic Editors: Leonor Maria and Joaquim Marçalo

Received: 1 February 2022

Accepted: 16 February 2022

Published: 18 February 2022

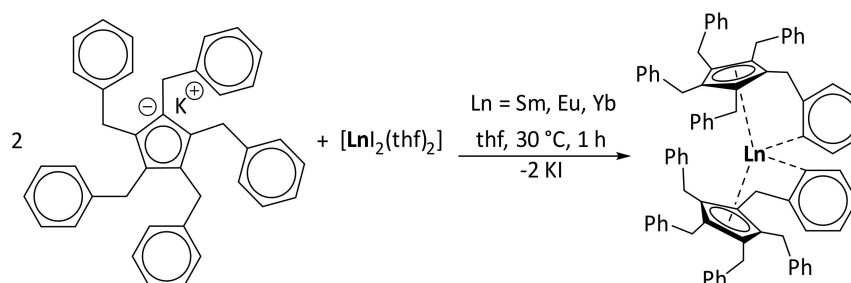
Publisher's Note: MDPI stays neutral with regard to jurisdictional claims in published maps and institutional affiliations.



Copyright: © 2022 by the authors. Licensee MDPI, Basel, Switzerland. This article is an open access article distributed under the terms and conditions of the Creative Commons Attribution (CC BY) license (<https://creativecommons.org/licenses/by/4.0/>).

1. Introduction

Pentabenzylcyclopentadiene ($\text{HCp}^{\text{Bz}5}$) was first synthesized by Hirsch and Bailey in 1978 [1]. In 1986, Rausch et al. reported the first metal complexes featuring a $\text{Cp}^{\text{Bz}5}$ ligand [2]. Subsequently, this ligand found use in the synthesis of a whole series of different complexes [3–5]. In 2015, Trifonov et al. synthesized the first divalent lanthanide complexes ligated by two $\text{Cp}^{\text{Bz}5}$ ligands, obtaining the corresponding divalent complexes $[\text{Cp}^{\text{Bz}5}_2\text{Ln}]$ with $\text{Ln} = \text{Eu}(\text{II}), \text{Yb}(\text{II})$ and $\text{Sm}(\text{II})$. Due to the sterically demanding ligand, as well as the saturated coordination sphere of the lanthanides by π -interaction with one phenyl ring per ligand, these compounds are present without any coordinating solvent at the metal center (Scheme 1) [6]. Lewis base adducts with simultaneous abolition of the metal–phenyl π -interactions could not be obtained even by specific reaction with donor molecules such as THF, DME, PMe_3 , or TMEDA. Consequently, this inertness can serve as indirect evidence for relatively strong $\text{Ln}(\text{II})$ -Ph π -interactions [6].



Scheme 1. Synthesis of $[\text{Cp}^{\text{Bz}5}_2\text{Ln}]$ with $\text{Ln} = \text{Sm}, \text{Eu}, \text{Yb}$ according to Trifonov et al. [6].

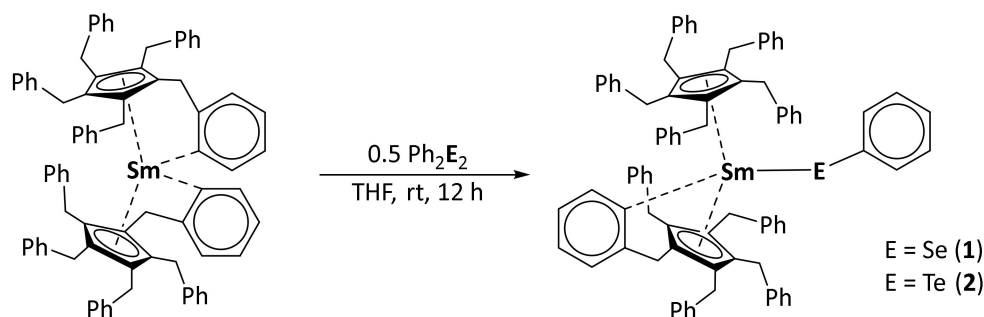
Moreover, since substituents on Cp rings are known to have an influence on the reactivity of corresponding lanthanoidocenes [7], the reactivity towards small molecules (H_2 , SiH_4 , N_2 , CO) and organic molecules with C-C multiple bonds (e.g., $\text{CH}_2=\text{CH}_2$, $\text{PhCH}=\text{CH}_2$,

trans-PhCH=CHPh, PhC≡CPh, Me₃SiC≡CSiMe₃) was also investigated. Surprisingly, no reactivity was detected towards any of these molecules [6]. This observation is particularly noteworthy for [Cp^{Bz5}₂Sm], since [Cp*₂Sm] (Cp* = pentamethylcyclopentadienyl) is shown to be reactive towards some of these compounds (e.g., N₂) [8]. The only reactivity observed for this new group of lanthanoidocenes was the reduction of bipyridine and phenazine by the samarium compound [6]. Thus, the coordination of the divalent lanthanides (Sm, Eu, Yb) with two Cp^{Bz5} ligands results in a remarkable stabilization of the otherwise much more reactive Ln(II) centers, which can be attributed to steric effects and their π-interaction with the benzyl groups of the ligands [6,9]. Based on this, the present work deals with the reactivity and stability of [Cp^{Bz5}₂Sm] towards other readily reducible inorganic substrates, which have been successfully reduced by us in previous work using divalent samarium compounds, in order to gain deeper insights into the reactivity of [Cp^{Bz5}₂Sm] and the stabilization upon coordination with the sterically demanding Cp^{Bz5} ligand [10].

2. Results and Discussion

2.1. Reduction of Diphenyl Dichalcogenides with [Cp^{Bz5}₂Sm]

The first attempts were the reactions of [Cp^{Bz5}₂Sm] with Ph₂E₂ (E = Se, Te) (Scheme 2) [10]. Ph₂E₂ can be cleaved by twofold single-electron transfer (SET) to give the respective selenol- or tellurolates. These reactions proceed under an E-E bond cleavage and result in either bridged and bimetallic or monometallic complexes, depending on the ligands used [11–13]. The reaction of [Cp^{Bz5}₂Sm] with Ph₂E₂ (E = Se, Te) at room temperature in THF gave yellow-orange solutions from which crystals of the monometallic compounds [Cp^{Bz5}₂Sm(SePh)] (1) and [Cp^{Bz5}₂Sm(TePh)] (2) were obtained by evaporation of *n*-pentane (Scheme 2). Compound 1 crystallizes with one molecule of the complex and one molecule of *n*-pentane in the asymmetric unit. Compound 2 crystallizes without any solvent molecule and with two molecules of 2 in the asymmetric unit (Figure 1). Due to the change in the oxidation state of the samarium atom from +II to +III and the associated smaller ionic radius (1.10 Å for Sm(III) and 1.36 Å for Sm(II)) [14], as well as the higher Lewis acidity, the Sm-Cp(Ctr) (Ctr = centroid) distances for 1 and 2 (2.4628(4) Å for 1 and 2.4583(6) Å for 2) are about 0.1 Å shorter than to those in [Cp^{Bz5}₂Sm] (2.565(1) Å) [6]. As a result of the [PhSe][−] resp. [PhTe][−] coordination, the metallocene angle, Cp(Ctr)-Ln-Cp(Ctr) of 1 and 2, is smaller than in [Cp^{Bz5}₂Sm] (139.67(2) (1) and 139.43(3) (2) vs. 141.8° in [Cp^{Bz5}₂Sm]) [6]. While in the divalent compound, [Cp^{Bz5}₂Sm] interactions with one phenyl ring of each Cp^{Bz5} ligand with the samarium atom can be observed, in 1 and 2, these are only observed for one phenyl ring in total, although a second phenyl ring is still oriented towards Sm, respectively. The resulting distances of 3.077(7) Å (for Sm-C18 in 1) and 3.007(3) Å (Sm-C68 in 2) are in the range of those observed for [Cp^{Bz5}₂Sm] (2.99–3.16 Å) [6].



Scheme 2. Reduction of Ph₂E₂ (E = Se, Te) with [Cp^{Bz5}₂Sm].

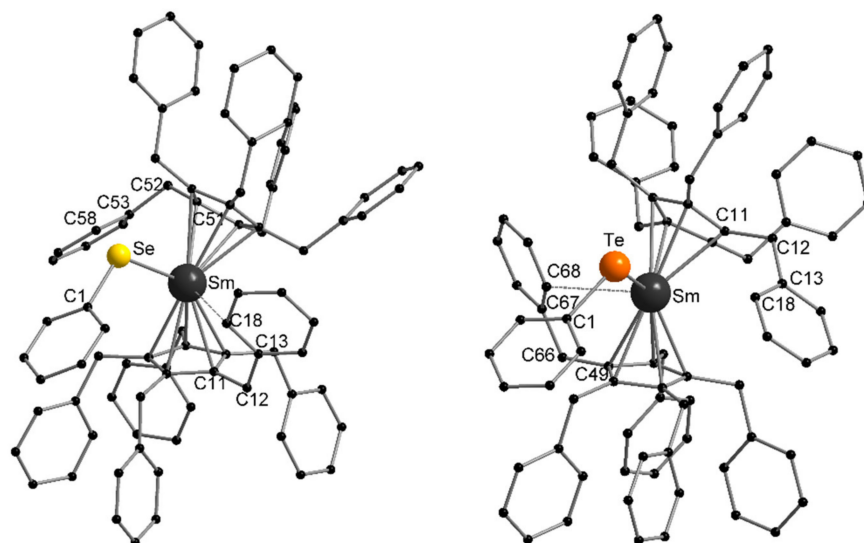


Figure 1. Molecular structures of **1** (left) and **2** (right) in the solid state. Hydrogen atoms and solvent molecules are omitted for clarity. Selected bond lengths [Å] and angles [°]: **1**: Sm–Se 2.8679(8), Sm–Cp(ctr) 2.4628(4), Sm–C18 3.077(7), Sm–C58 3.712(8), Se–C1 1.929(8), Sm–Se–C1 111.7(2), C11–C12–C13 114.8(7), C51–C52–C53 118.6(7), Cp(ctr)–Sm–Cp(ctr) 139.67(2). **2**: Sm–Te 3.1186(2), Sm–Cp(ctr) 2.4583(6), Sm–C68 3.007(3), Sm–C18 3.780(3), Te–C1 2.132(3), Sm–Te–C1 109.81(7), C49–C66–C67 114.5(2), C11–C12–C13 119.0(2), Cp(ctr)–Sm–Cp(ctr) 139.43(3).

Moreover, the interaction of the phenyl ring with the metal center also affects the angles in the ligand, resulting in a smaller Cp–C–phenyl angle (C11–C12–C13 114.8(7)° vs. C51–C52–C53 118.6(7)° for **1** and C49–C66–C67 114.5(2)° vs. C11–C12–C13 119.0(2)° for **2**). The distances to the other phenyl rings in each case are >3.7 Å, which is outside the range of possible interactions. Both the Sm–Se (2.8679(8) Å) and Sm–Te distances (3.1187(2) Å) are within the range of comparable compounds from the literature (Sm–Se 2.8837(6) Å for [(Cp*₂Sm)SePh(thf)] and Sm–Te 3.1279(3) Å for [(Cp*₂Sm)TePh(thf)] [11]. In contrast, the Sm–Se/Te–C1 angles of 111.7(2)° (**1**) and 109.81(7)° (**2**) are 6° (**1**) and 3° (**2**) smaller than in comparable compounds, e.g., 112.49(6)° in [(Cp*₂Sm)(TePh)(thf)] [11].

IR spectroscopic studies can also confirm the presence of monosubstituted aromatic rings (benzyl and EPh) in compounds **1** and **2** (Figures S1 and S2). Thus, the typical aromatic fingers (overtone and combination vibrations of the aromatic system) were detected as very weak bands between 1665 and 2000 cm^{−1}, and the relevant C–H out-of-plane (“oop”) motions were seen as intense bands (e.g., 731 and 693 cm^{−1} for **2**) [15]. Other bands were assigned to the “in-plane” C–H bending vibrations (1074 and 1029 cm^{−1}), the C–C stretching vibrations of the aromatic ring (1600–1570 cm^{−1}) and the C–H stretching vibrations of the alkyl groups (2910–2830 cm^{−1}) and aromatic rings (3085–3025 cm^{−1}) [15].

2.2. Reduction of d-Metal Carbonyl Complexes with [Cp^{Bz5}₂Sm]

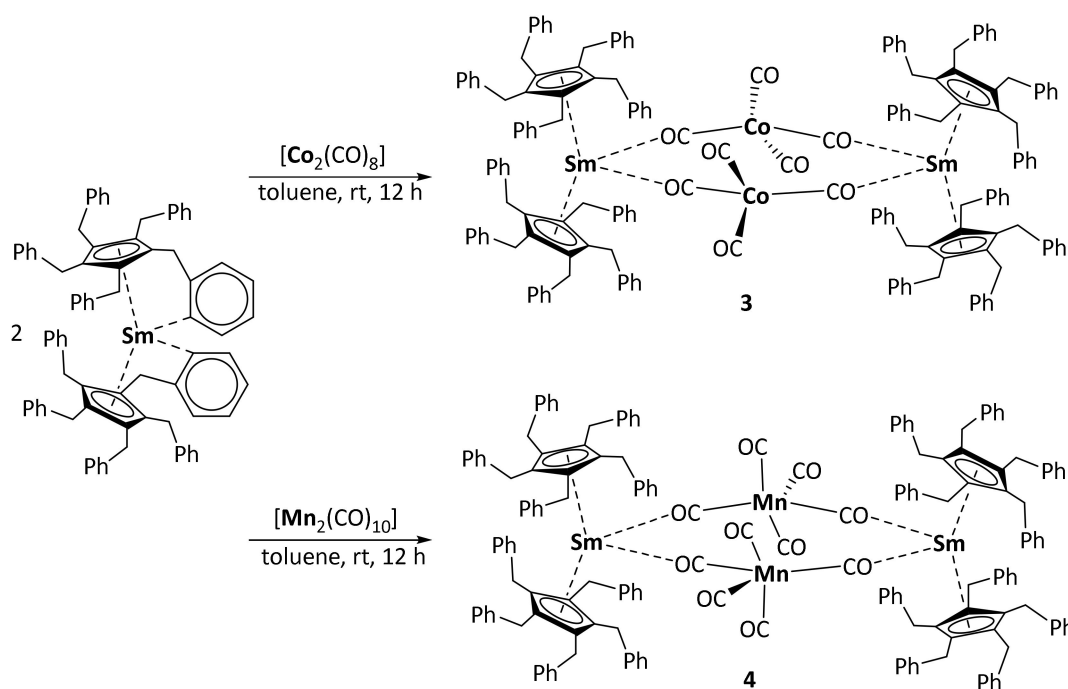
After the successful reaction of [Cp^{Bz5}₂Sm] with Ph₂E₂ (E = Se, Te), the reductions of d-metal carbonyl complexes were investigated [10].

The first structurally characterized d/f-element carbonyl complex [(Cp*₂Yb)₂(OC)₄{(CO)₇Fe₃] was obtained by Anderson et al. by the reduction of [Fe₂(CO)₉] with divalent [Cp*₂Yb(OEt₂)] [16]. In general, in these reactions a SET from Ln(II) to the d-metal carbonyl complex occurs, resulting in the formation of a [M(CO)_x] anion and, if given, cleavage of the M–M bond. In contrast, the formation of new M–M bonds is also possible. As a consequence of such reductive approaches, different structural motifs were reported. These include: (i) simple bimetallic complexes, (ii) bridging or polymeric structural motifs in which the Ln(III) fragments are usually coordinated to the [M(CO)_x] anions via carbonyl bridges and (iii) new anionic d-metal carbonyl clusters without any coordination of the

lanthanide ion to the carbonyl cluster [16–23]. In recent studies of our group, the steric influence of various ligands on the product formation in the reductive synthesis of such d/f-element carbonyl complexes has been specifically investigated for the first time [20,24]. In light of these observations, we felt challenged to study the reactivity of the super bulky samarocen $[\text{Cp}^{\text{Bz5}}_2\text{Sm}]$ with various d-metal carbonyl complexes.

The reaction of $[\text{Cp}^{\text{Bz5}}_2\text{Sm}]$ with $[\text{Co}_2(\text{CO})_8]$ or $[\text{Mn}_2(\text{CO})_{10}]$ in toluene gave the bridged tetrametallic complexes $[(\text{Cp}^{\text{Bz5}}_2\text{Sm})_2\{(\mu\text{-OC})_2\text{Co}(\text{CO})_2\}_2]$ (**3**) or $[(\text{Cp}^{\text{Bz5}}_2\text{Sm})_2\{(\mu\text{-OC})_2\text{Mn}(\text{CO})_3\}_2]$ (**4**) (Scheme 3). The formation of these compounds can be explained by twofold SET towards the d-metal carbonyl groups, resulting in cleavage of the metal–metal bond. Subsequently, the resulting tetracarbonyl cobaltate or pentacarbonyl manganate anions coordinate to two, now trivalent, Sm atoms of the $[\text{Cp}^{\text{Bz5}}_2\text{Sm}]^+$ units in a bridging bonding mode. Complexes **3** and **4** both crystallize with half a molecule of the respective compound and two (**3**) or three and a half (**4**) molecules of toluene in the asymmetric unit (Figures 2 and 3). In contrast to compounds **1** and **2**, compounds **3** and **4** feature only one phenyl ring per $[\text{Cp}^{\text{Bz5}}_2\text{Sm}]^+$ unit oriented towards the Sm atom, while all other benzyl moieties are rotated away from the latter. This is a result of the bulkier bridging carbonyl metallate anions.

The Sm–phenyl distances observed here are above 3.8 Å for both **3** (Sm1–C80 3.828(3) Å) and **4** (Sm1–C13 3.835(8) Å), so no Sm–phenyl interactions occur. The Sm–Cp distances are further shortened compared to **1** and **2** (**3**: Sm1–Cp(Ctr) 2.4080(4)/2.4156(5) Å, **4**: Sm1–Cp(Ctr) 2.4214(4)/2.4410(4) Å), while the Cp–Sm–Cp angles are increasingly widened (**3**: 144.95(2)°, **4**: 141.71(2)°). The Sm–O distances in **3** are 2.394(2) and 2.416(2) Å and thus comparable to 2.409(5) and 2.424(5) Å in **4**. The tetracarbonyl cobaltate anions in **3** occur in a distorted tetrahedral geometry with C–Co–C angles between 113.72(12) and 104.88(13)°. Due to the coordination of O1 and O2 to the $[\text{Cp}^{\text{Bz5}}_2\text{Sm}]^+$ moieties and the resulting decreased electron density in the highest occupied molecular orbital (HOMO) of the corresponding carbonyl groups, the O–C bond lengths in these are longer than in the terminal ones (O3–C3 1.131(4) Å, O4–C4 1.137(4) Å), at 1.173(3) Å.



Scheme 3. Synthesis of $[(\text{Cp}^{\text{Bz5}}_2\text{Sm})_2\{(\mu\text{-OC})_2\text{Co}(\text{CO})_2\}_2]$ (**3**) and $[(\text{Cp}^{\text{Bz5}}_2\text{Sm})_2\{(\mu\text{-OC})_2\text{Mn}(\text{CO})_3\}_2]$ (**4**).

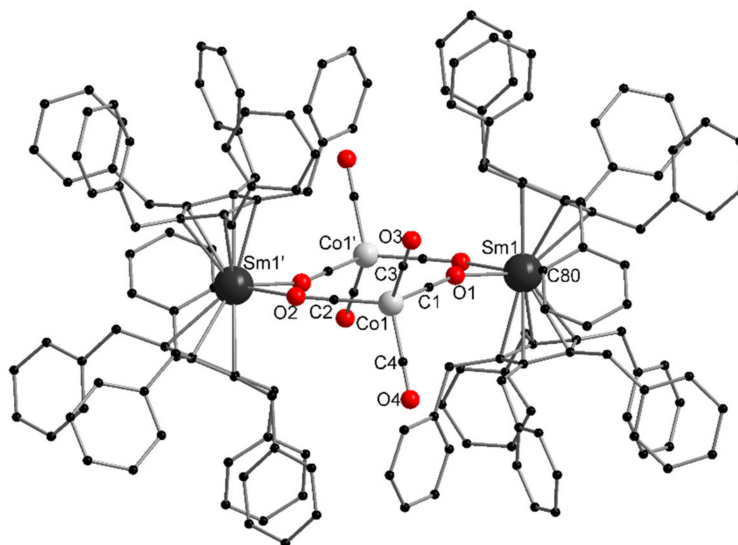


Figure 2. Molecular structure of **3** in the solid state. Hydrogen atoms and solvent molecules are omitted for clarity. Selected bond lengths [Å] and angles [°]: Sm1-O1 2.394(2), Sm1-O2' 2.416(2), Sm1-Cp(Ctr) 2.4080(4)/2.4156(5), Sm1-C80 3.828(3), Co1-C1 1.719(3), Co1-C2 1.723(2), Co1-C3 1.790(3), Co1-C4 1.801(3), O1-C1 1.173(3), O2-C2 1.173(3), O3-C3 1.131(4), O4-C4 1.137(4), O1-Sm1-O2' 75.65(7), Cp(Ctr)-Sm1-Cp(Ctr) 144.95(2), C1-Co1-C2 113.72(12), C1-Co1-C3 104.88(13), C1-Co1-C4 109.05(13), C3-Co1-C2 111.07(13), C3-Co1-C4 109.51(13), C4-Co1-C2 108.52(12).

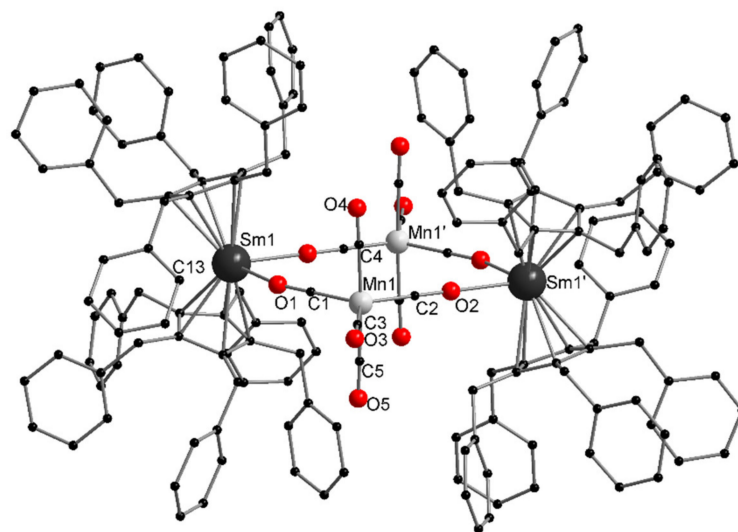


Figure 3. Molecular structure of **4** in the solid state. Hydrogen atoms and solvent molecules are omitted for clarity. Selected bond lengths [Å] and angles [°]: Sm1-O1 2.409(5), Sm1-O2' 2.424(5), Sm1-Cp(Ctr) 2.4214(4)/2.4410(4), Sm1-C13 3.835(8), Mn1-C1 1.767(8), Mn1-C2 1.765(8), Mn1-C3 1.838(9), Mn1-C4 1.848(9), Mn1-C5 1.827(9), O1-C1 1.169(9), O2-C2 1.197(9), O3-C3 1.146(10), O4-C4 1.150(10), O5-C5 1.165(11), O1-Sm1-O2' 76.8(2), Cp(Ctr)-Sm1-Cp(Ctr) 141.71(2), C1-Mn1-C2 121.8(3), C1-Mn1-C3 120.0(4), C1-Mn1-C4 89.5(4), C1-Mn1-C5 89.5(4), C2-Mn1-C3 118.2(4), C2-Mn1-C4 93.4(3), C2-Mn1-C5 89.8(3), C3-Mn1-C4 89.7(4), C3-Mn1-C5 88.4(4).

The Co-C bond lengths are also affected by the different carbonyl functions (bridging vs. terminal). Thus, these are shortened for the bridging carbonyl groups (Co1-C1 1.719(3) Å, Co1-C2 1.723(2) Å) compared to the terminal ones (Co1-C3 1.790(3) Å, Co1-C4 1.801(3) Å).

In compound **4**, the pentacarbonyl manganese anion forms a slightly distorted trigonal-bipyramidal coordination polyhedron. As a result, the angles between the equatorial carbonyl groups are all close to 120° (C1-Mn1-C2 121.8(3)°, C1-Mn1-C3 120.0(4)°, C2-

Mn1-C3 118. 2(4)°), while the angles between these and the axial ones are close to 90° (C1-Mn1-C4 89.5(4)°, C1-Mn1-C5 89.5(4)°, C2-Mn1-C4 93.4(3)°, C2-Mn1-C5 89.8(3)°, C3-Mn1-C4 89.7(4)°, C3-Mn1-C5 88.4(4)°). Analogous to **3**, also in **4**, the C-O bonds of the bridging carbonyl groups (O1-C1 1.169(9) Å, O2-C2 1.197(9) Å) are longer than in the terminal ones. In addition, the C-O bond of the single terminal equatorial carbonyl group is significantly longer than in the axial ones (O5-C5 1.165(11) Å (O5-C5) vs. 1.146(10) and 1.150(10) Å (O3-C3, O4-C4)). The Mn-C bonds are also shortened for C1 and C2 (1.767(8), 1.765(8) Å) compared to those of C3-5 (1.838(9), 1.848(9) and 1.827(9) Å) due to the bonding of the associated carbonyl groups to the Sm(III) unit.

The presence of bridging and terminal carbonyl groups in **3** and **4** can also be confirmed by IR measurements (Figures S3 and S4). In the corresponding spectra, the aromatic fingers observed for **1** and **2** are overlaid by strong bands of carbonyl stretching vibrations. For **3**, this results in two bands at 2038 and 1972 cm⁻¹, which can be assigned to the terminal carbonyl groups by literature comparison (e.g., with [NMe₃H][Co(CO)₄]) [25]. The other two bands at 1814 and 1783 cm⁻¹ are shifted towards lower wavenumbers and can accordingly be assigned to the bridging carbonyl groups. These observations are consistent with other d/f-element carbonyl complexes in the literature [16,18]. The remaining observed bands in the IR spectrum of **3** are in agreement with the expected bands for the Cp^{Bz5} ligand. For **4**, a comparable IR spectrum is obtained with several bands each for the terminal (from ca. 2006 to 1896 cm⁻¹) and bridging (ca. 1814 to 1784 cm⁻¹) carbonyl groups.

Compound **3** thus represents only the second example of such a heterometallic Sm-Co carbonyl complex, in which two Sm(III) units are bridged via the carbonyl groups of two tetracarbonyl cobaltate anions, after [((DippForm)₂Sm(thf))₂{(μ-OC)₂Co(CO)₂}₂] presented by us in 2020 [24]. In other previously reported reactions of divalent Sm compounds with cobalt carbonyl complexes, unbridged structural motifs or separated ion pairs were obtained [26,27]. Bridging of two Sm units by a pentacarbonyl manganate anion has previously been observed only for the polymeric species [((Cp*)₂Sm(thf))₂{(μ-OC)₂[Mn(CO)₃]}_n] [20]. In other cases, only unbridged structural motifs or separated ion pairs were obtained [20,28], making **4** the first example of such a tetrametallic Mn-Sm complex with isocarbonyl bridges.

3. Experimental Section

3.1. Materials and Methods

All manipulations of water- and air-sensitive compounds were performed with exclusion of moisture and oxygen in flame-dried Schlenk-type glassware either on a dual-manifold Schlenk line, interfaced to a high vacuum (10⁻³ mbar) line, or in an argon-filled MBraun glove box. Tetrahydrofuran and benzene were distilled under nitrogen from potassium benzophenoneketyl before storage in vacuo over LiAlH₄. Hydrocarbon solvents were dried by using an MBraun solvent purification system (SPS 800), degassed and stored in vacuo over LiAlH₄.

Elemental analyses were carried out with an Elementar Vario Micro cube. IR spectra were obtained on a Bruker Tensor 37 spectrometer equipped with a room temperature DLATGS detector and a diamond ATR (attenuated total reflection) unit. SmI₂*(thf)₂ [29], HCp^{Bz5} [2], KCp^{Bz5} [5] and [Cp^{Bz5}₂Sm] [6] were prepared following literature procedures.

General remark: No meaningful NMR spectra could be obtained due to the paramagnetic nature of Sm.

3.2. Synthesis of Complexes

[Cp^{Bz5}₂Sm(SePh)] (**1**) [10]: THF (8 mL) was added to a mixture of 60.0 mg (0.05 mmol, 1 eq.) [Cp^{Bz5}₂Sm] and 7.9 mg (0.025 mmol, 0.5 eq.) Ph₂Se₂. The resulting reaction mixture was stirred at room temperature for 12 h, and the resulting orange solution was filtered. Single crystals of **1****n*-pentane suitable for X-ray structural analysis were obtained by slow evaporation of *n*-pentane into a concentrated THF solution. Crystalline yield: 25 mg (37%).

IR (ATR): $\tilde{\nu}$ [cm^{-1}] = 3059 (m), 3025 (m), 2904 (w), 2834 (vw), 1947 (vw), 1876 (vw), 1801 (vw), 1600 (m), 1575 (m), 1492 (s), 1468 (m), 1449 (s), 1418 (w), 1241 (br,w), 1181 (w), 1153 (w), 1069 (m), 1028 (m), 983 (w), 907 (vw), 841 (vw), 794 (vw), 733 (s), 693 (vs), 666 (w), 614 (vw), 584 (w), 551 (vw), 473 (m).

Elemental analysis: calculated (%) for $[\text{C}_{86}\text{H}_{75}\text{SeSm}]$ (1337.8 g/mol): C 77.21, H 5.65; found: C 76.32, H 5.75.

$[\text{Cp}^{\text{Bz}5}_2\text{Sm}(\text{TePh})]$ (2) [10]: THF (10 mL) was added to a mixture of 83.0 mg (0.07 mmol, 1 eq.) $[\text{Cp}^{\text{Bz}5}_2\text{Sm}]$ and 14.37 mg (0.035 mmol, 0.5 eq.) Ph_2Te_2 . The resulting reaction mixture was stirred at room temperature for 12 h, and the resulting orange solution was filtered. Single crystals of 2 suitable for X-ray structural analysis were obtained by slow evaporation of *n*-pentane into a concentrated THF solution. Crystalline yield: 50 mg (52%).

IR (ATR): $\tilde{\nu}$ [cm^{-1}] = 3082 (w), 3059 (m), 3025 (m), 2905 (w), 2835 (vw), 1946 (vw), 1874 (vw), 1803 (vw), 1600 (m), 1570 (w), 1492 (s), 1468 (m), 1450 (s), 1433 (m), 1325 (vw), 1261 (vw), 1181 (vw), 1153 (vw), 1074 (w), 1029 (w), 1017 (w), 996 (vw), 906 (vw), 794 (vw), 731 (vs), 693 (vs), 613 (vw), 583 (vw), 473 (w), 455 (w).

Elemental analysis: calculated (%) for $[\text{C}_{86}\text{H}_{75}\text{TeSm}]$ (1386.51 g/mol): C 74.50, H 5.45; found: C 73.91, H 5.47.

$[(\text{Cp}^{\text{Bz}5}_2\text{Sm})_2\{(\mu\text{-OC})_2\text{Co}(\text{CO})_2\}_2]$ (3) [10]: Toluene (10 mL) was added to a mixture of 60.0 mg (0.05 mmol, 1 eq.) $[\text{Cp}^{\text{Bz}5}_2\text{Sm}]$ and 8.55 mg (0.025 mmol, 0.5 eq.) $[\text{Co}_2(\text{CO})_8]$. The resulting reaction mixture was stirred for 12 h at room temperature. Single crystals of 3*2 toluene suitable for X-ray structural analysis were obtained by cooling a concentrated toluene solution to -35°C . Crystalline yield: 30 mg (44%).

IR (ATR): $\tilde{\nu}$ [cm^{-1}] = 3084 (vw), 3061 (w), 3025 (w), 2907 (vw), 2038 (m), 1972 (s), 1814 (s), 1783 (vs), 1601 (w), 1493 (m), 1451 (m), 1327 (vw), 1180 (vw), 1075 (w), 1029 (w), 730 (m), 694 (s), 614 (vw), 567 (w), 511 (w), 477 (w).

Elemental analysis: calculated (%) for $[\text{C}_{168}\text{H}_{140}\text{Co}_2\text{O}_8\text{Sm}_2]$ (2705.55 g/mol): C 74.58, H 5.22; found: The values found were reproducibly too low due to carbide formation.

$[(\text{Cp}^{\text{Bz}5}_2\text{Sm})_2\{(\mu\text{-OC})_2\text{Mn}(\text{CO})_3\}_2]$ (4) [10]: Toluene (5 mL) was added to a mixture of 66.0 mg (0.056 mmol, 1 eq.) $[\text{Cp}^{\text{Bz}5}_2\text{Sm}]$ and 10.9 mg (0.028 mmol, 0.5 eq.) $[\text{Mn}_2(\text{CO})_{10}]$, and the resulting reaction mixture was stirred for 12 h at room temperature. Then, the obtained suspension was carefully heated until a clear solution was obtained. Single crystals of 4*7 toluene suitable for X-ray structural analysis were obtained by subsequent cooling to -35°C . Crystalline yield: 30 mg (39 %).

IR (ATR): $\tilde{\nu}$ [cm^{-1}] = 3083 (w), 3060 (m), 3025 (m), 2917 (br,m), 2851 (w), 2006 (vs), 1972 (vs), 1944 (vs), 1896 (w), 1814 (s), 1784 (s), 1652 (vw), 1600 (m), 1540 (w), 1493 (vs), 1451 (s), 1325 (vw), 1181 (vw), 1155 (vw), 1074 (m), 1029 (m), 982 (vw), 902 (vw), 842 (vw), 730 (s), 694 (vs), 611 (vw), 547 (w), 512 (w), 476 (w), 418 (vw).

Elemental analysis: calculated (%) for $[\text{C}_{170}\text{H}_{140}\text{Mn}_2\text{O}_{10}\text{Sm}_2]$ (2753.58 g/mol): C 74.15, H 5.12; found: The values found were reproducibly too low due to carbide formation.

3.3. Single-Crystal X-ray Crystallography Data Collection and Refinement

A suitable crystal was covered in mineral oil (Aldrich) and mounted on a glass fiber. The crystal was transferred directly to the cold stream of a STOE IPDS 2 or a STOE StadiVari diffractometer. All structures were solved by using the program SHELXS/T [30–32] and Olex2 [33]. The remaining non-hydrogen atoms were located from successive difference Fourier map calculations. The refinements were carried out by using full-matrix least-squares techniques on F^2 by using the program SHELXL [30,31]. In each case, the locations of the largest peaks in the final difference Fourier map calculations, as well as the magnitude of the residual electron densities, were of no chemical significance. Further details are given in Table S1.

Crystallographic data (excluding structure factors) for the structures reported in this paper have been deposited with the Cambridge Crystallographic Data Centre as a Supplementary Materials (No. 2149615–2149618). Copies of the data can be obtained

free of charge on application to CCDC, 12 Union Road, Cambridge CB21EZ, UK (fax: +(44)1223-336-033; email: deposit@ccdc.cam.ac.uk).

4. Conclusions

In the present work, it was shown that the super bulky divalent lanthanide compound $[\text{Cp}^{\text{Bz5}}_2\text{Sm}]$ is more reactive than suggested by the initial studies of Trifonov et al. [6]. Thus, the title compound could be used in various redox reactions both for the reduction of diphenyl dichalcogenides and for the reductive synthesis of d/f-element carbonyl complexes. While the products obtained in the former reaction form monometallic complexes (1, 2), tetrametallic bridged compounds were obtained for the d/f-element carbonyl complexes (3, 4). In all new compounds, a different number of Sm-C(phenyl) interactions and also differently oriented benzyl moieties were observed, suggesting—despite the preference of these interactions in $[\text{Cp}^{\text{Bz5}}_2\text{Sm}]$ described by Trifonov et al.—a flexible orientation of these moieties and thus a variable steric shielding of the metal center by the ligand.

Supplementary Materials: The following supporting information can be downloaded at: <https://www.mdpi.com/article/10.3390/inorganics10020025/s1>, Figures S1–S4: IR Spectra of compounds 1–4; Table S1: Crystal data and structure refinement of 1, 2, 3 and 4.

Author Contributions: N.R. conducted the experimental work and conducted X-ray experiments. P.W.R. originated the idea, supervised the work and interpreted the results. All authors have read and agreed to the published version of the manuscript.

Funding: N.R.'s Ph.D. study is additionally funded by the Fonds der Chemischen Industrie (102431). Financial support by the DFG-funded transregional collaborative research center SFB/TRR 88 “Cooperative Effects in Homo and Heterometallic Complexes (3MET)” project B3 is gratefully acknowledged.

Institutional Review Board Statement: Not applicable.

Informed Consent Statement: Not applicable.

Data Availability Statement: Spectroscopic data and detailed crystallographic information can be found in the Supplementary Materials. Crystallographic data are available via the Cambridge Crystallographic Data Centre (CCDC): 2149615–2149618.

Acknowledgments: We thank C. Schoo for his help in solving the crystal structures.

Conflicts of Interest: The authors declare no conflict of interest.

References

1. Hirsch, S.S.; Bailey, W.J. Base-catalyzed alkylation of cyclopentadiene rings with alcohols and amines. *J. Org. Chem.* **1978**, *43*, 4090–4094. [[CrossRef](#)]
2. Chambers, J.W.; Baskar, A.J.; Bott, S.G.; Atwood, J.L.; Rausch, M.D. Formation and molecular structures of (η -5-pentabenzylcyclopentadienyl)- and (η -5-pentaphenylcyclopentadienyl)dicarbonyl derivatives of cobalt and rhodium. *Organometallics* **1986**, *5*, 1635–1641. [[CrossRef](#)]
3. Tsai, W.-M.; Rausch, M.D.; Rogers, R.D. Improved Synthesis of Pentabenzylcyclopentadiene and Study of the Reaction between Pentabenzylcyclopentadiene and Iron Pentacarbonyl. *Organometallics* **1996**, *15*, 2591–2594. [[CrossRef](#)]
4. Delville-Desbois, M.-H.; Mross, S.; Astruc, D. Chemistry of (Pentabenzylcyclopentadienyl)iron Compounds Including 17-Electron Dithiocarbamate Complexes. *Organometallics* **1996**, *15*, 5598–5604. [[CrossRef](#)]
5. Schumann, H.; Janiak, C.; Köhn, R.D.; Loebel, J.; Dietrich, A. Synthesis and structure of $\text{Fe}[\text{C}_5(\text{CH}_2\text{Ph})_5]_2$ and $\text{Lu}(\text{C}_8\text{H}_8)[\text{C}_5(\text{CH}_2\text{Ph})_5]$. *J. Organomet. Chem.* **1989**, *365*, 137–150. [[CrossRef](#)]
6. Selikhov, A.N.; Mahrova, T.V.; Cherkasov, A.V.; Fukin, G.K.; Larionova, J.; Long, J.; Trifonov, A.A. Base-Free Lanthanoidocenes(II) Coordinated by Bulky Pentabenzylcyclopentadienyl Ligands. *Organometallics* **2015**, *34*, 1991–1999. [[CrossRef](#)]
7. Schultz, M.; Boncella, J.M.; Berg, D.J.; Tilley, T.D.; Andersen, R.A. Coordination of 2,2'-Bipyridyl and 1,10-Phenanthroline to Substituted Ytterbocenes: An Experimental Investigation of Spin Coupling in Lanthanide Complexes. *Organometallics* **2002**, *21*, 460–472. [[CrossRef](#)]
8. Szostak, M.; Procter, D.J. Beyond Samarium Diiodide: Vistas in Reductive Chemistry Mediated by Lanthanides(II). *Angew. Chem. Int. Ed.* **2012**, *51*, 9238–9256. [[CrossRef](#)]
9. Bochkarev, M.N. Synthesis, Arrangement, and Reactivity of Arene–Lanthanide Compounds. *Chem. Rev.* **2002**, *102*, 2089–2118. [[CrossRef](#)]

10. Reinfandt, N. Untersuchungen zur Reaktivität klassischer und Nicht-Klassischer Divalenter Lanthanoidverbindungen Gegenüber Pnictogenen und deren Verbindungen Sowie Darstellung Heterobimetallischer Lanthanoid-Münzmetallkomplexe. Ph.D. Thesis, Karlsruher Institut für Technologie, Karlsruhe, Germany, 2021.
11. Evans, W.J.; Miller, K.A.; Lee, D.S.; Ziller, J.W. Synthesis, Structure, and Ligand-Based Reduction Reactivity of Trivalent Organosamarium Benzene Chalcogenolate Complexes $(C_5Me_5)_2Sm(EPh)(THF)$ and $[(C_5Me_5)_2Sm(\mu-EPh)]_2$. *Inorg. Chem.* **2005**, *44*, 4326–4332. [[CrossRef](#)]
12. Hillier, A.C.; Liu, S.-Y.; Sella, A.; Elsegood, M.R.J. Lanthanide Chalcogenolate Complexes: Synthesis and Crystal Structures of the Isoleptic Series $[Sm(TpMe,Me)_2ER]$ (E = O, S, Se, Te; TpMe,Me = tris-3,5-Dimethylpyrazolylborate). *Inorg. Chem.* **2000**, *39*, 2635–2644. [[CrossRef](#)] [[PubMed](#)]
13. Evans, W.J.; Miller, K.A.; Ziller, J.W. Synthesis of $(O_2CEPh)^{1-}$ Ligands (E = S, Se) by CO_2 Insertion into Lanthanide Chalcogen Bonds and Their Utility in Forming Crystallographically Characterizable Organoaluminum Complexes $[Me_2Al(\mu-O_2CEPh)]_2$. *Inorg. Chem.* **2006**, *45*, 424–429. [[CrossRef](#)] [[PubMed](#)]
14. Hollemann, A.F.; Wiberg, E.; Wiberg, N. *Lehrbuch der Anorganischen Chemie*; Walter de Gruyter & Co.: Berlin, Germany, 2007.
15. Pretsch, E.; Bühlmann, P.; Badertscher, M. *Spektroskopische Daten Zur Strukturklärung Organischer Verbindungen*, 5th ed.; Springer: Berlin/Heidelberg, Germany, 2010.
16. Tilley, T.D.; Andersen, R.A. Preparation and crystal structure of μ -carbonyl-OC-bis(pentamethylcyclopentadienyl)(tetrahydrofuran) ytterbium(III)tricarbonylcobalt(I); A Yb-OC-Co linkage. *J. Chem. Soc. Chem. Commun.* **1981**, 985–986. [[CrossRef](#)]
17. Tilley, T.D.; Andersen, R. Preparation and crystal structure of bis[bis(pentamethylcyclopentadienyl)ytterbium(III)] undecacarbonyltriferrate, $[(C_5Me_5)_2Yb]_2[Fe_3(CO)_{11}]$; a compound with four isocarbonyl (iron-carbonyl-ytterbium) interactions. *J. Am. Chem. Soc.* **1982**, *104*, 1772–1774. [[CrossRef](#)]
18. Boncella, J.M.; Andersen, R.A. Bis(pentamethylcyclopentadienyl)ytterbium(II) as a Lewis acid and electron-transfer ligand. Preparation and crystal structures of $[Yb(Me_5C_5)_2(\mu-CO)_xMn(CO)_{5-x}]_y$ (x, y = 2; x = 3, y = ∞). *Inorg. Chem.* **1984**, *23*, 432–437. [[CrossRef](#)]
19. Recknagel, A.; Steiner, A.; Brooker, S.; Stalke, D.; Edelmann, F.T. $[Cp_2^*Sm(\mu-OC)_2FeCp^*]_2$. *Chem. Ber.* **1991**, *124*, 1373–1375. [[CrossRef](#)]
20. Yadav, R.; Simler, T.; Gamer, M.T.; Köppe, R.; Roesky, P.W. Rhenium is different: CO tetramerization induced by a divalent lanthanide complex in rhenium carbonyls. *Chem. Commun.* **2019**, *55*, 5765–5768. [[CrossRef](#)]
21. Boncella, J.M.; Andersen, R.A. Preparation of $[(Yb(C_5Me_5)_2)_2\{Co_3(C_5H_4R)_2(\mu_3-CO)_4\}]$, R = H, Me, SiMe₃; an example of a 47-electron transition metal fragment containing a cobalt atom with hexagonal planar co-ordination. *J. Chem. Soc. Chem. Commun.* **1984**, 809–810. [[CrossRef](#)]
22. Deacon, G.B.; Guo, Z.; Junk, P.C.; Wang, J. Reductive Trapping of $[(OC)_5W-W(CO)_5]^{2-}$ in a Mixed-Valent SmII/III Calix[4]pyrrolide Sandwich. *Angew. Chem. Int. Ed.* **2017**, *56*, 8486–8489. [[CrossRef](#)]
23. Hillier, A.C.; Sella, A.; Elsegood, M.R.J. Reduction of rhenium decacarbonyl by samarium(II): Synthesis and structure of the spiked triangular anion $[HRe_4(CO)_{17}]^-$. *J. Organomet. Chem.* **1999**, *588*, 200–204. [[CrossRef](#)]
24. Yadav, R.; Hossain, M.E.; Peedika Paramban, R.; Simler, T.; Schöo, C.; Wang, J.; Deacon, G.B.; Junk, P.C.; Roesky, P.W. 3d–4f heterometallic complexes by the reduction of transition metal carbonyls with bulky LnII amidinates. *Dalton Trans.* **2020**, *49*, 7701–7707. [[CrossRef](#)] [[PubMed](#)]
25. Calderazzo, F.; Fachinetti, G.; Marchetti, F.; Zanazzi, P.F. Preparation and crystal and molecular structure of two trialkylamine adducts of $HCo(CO)_4$ showing a preferential $NR_3H + [(OC)_3Co(CO)]^-$ interaction. *J. Chem. Soc., Chem. Commun.* **1981**, 181–183. [[CrossRef](#)]
26. Evans, W.J.; Bloom, I.; Grate, J.W.; Hughes, L.A.; Hunter, W.E.; Atwood, J.L. Synthesis and characterization of the samarium-cobalt complexes $(C_5Me_5)_2(THF)SmCo(CO)_4$ and $(SmI_2(THF)_5)(Co(CO)_4)$: X-ray crystal structure of a seven-coordinate samarium(III) cation complex. *Inorg. Chem.* **1985**, *24*, 4620–4623. [[CrossRef](#)]
27. Blake, M.P.; Kaltsoyannis, N.; Mountford, P. Probing the Limits of Alkaline Earth–Transition Metal Bonding: An Experimental and Computational Study. *J. Am. Chem. Soc.* **2015**, *137*, 12352–12368. [[CrossRef](#)] [[PubMed](#)]
28. Hillier, A.C.; Sella, A.; Elsegood, M.R.J. The reaction of samarium(II) with manganese carbonyl: Unexpected conversion of CO to formate. X-ray crystal structures of $[Sm(TpMe_2)_2]Mn(CO)_5$ and $[(Sm(TpMe_2)_2)_2(\mu-HCO_2)]Mn(CO)_5$ (TpMe₂=HB(3,5-dimethylpyrazolyl)). *J. Organomet. Chem.* **2002**, *664*, 298–305. [[CrossRef](#)]
29. Girard, P.; Namy, J.L.; Kagan, H.B. Divalent lanthanide derivatives in organic synthesis. 1. Mild preparation of samarium iodide and ytterbium iodide and their use as reducing or coupling agents. *J. Am. Chem. Soc.* **1980**, *102*, 2693–2698. [[CrossRef](#)]
30. Sheldrick, G. A short history of SHELX. *Acta Crystallogr. Sect. A* **2008**, *64*, 112–122. [[CrossRef](#)]
31. Sheldrick, G. Crystal structure refinement with SHELXL. *Acta Crystallogr. Sect. C* **2015**, *71*, 3–8. [[CrossRef](#)]
32. Sheldrick, G. SHELXT—Integrated space-group and crystal-structure determination. *Acta Crystallogr. Sect. A* **2015**, *71*, 3–8. [[CrossRef](#)]
33. Dolomanov, O.V.; Bourhis, L.J.; Gildea, R.J.; Howard, J.A.K.; Puschmann, H. OLEX2: A complete structure solution, refinement and analysis program. *J. Appl. Crystallogr.* **2009**, *42*, 339–341. [[CrossRef](#)]